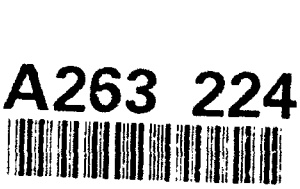

ARMY RESEARCH LABORATORY

Influence of Ply Waviness on Stiffness and Strength Reduction of Composite Laminates

Travis A. Bogetti
U.S. ARMY RESEARCH LABORATORY

Jack W. Gillespie, Jr.
UNIVERSITY OF DELAWARE

Mark A. Lamontia
E. I. DUPONT DE NEMOURS AND COMPANY, INC.

ARL-TR-110 April 1993

NOTICES

Destroy this report when it is no longer needed. DO NOT return it to the originator.

Additional copies of this report may be obtained from the National Technical Information Service, U.S. Department of Commerce, 5285 Port Royal Road, Springfield, VA 22161.

The findings of this report are not to be construed as an official Department of the Army position, unless so designated by other authorized documents.

The use of trade names or manufacturers' names in this report does not constitute indorsement of any commercial product.

REPORT DOCUMENTATION PAGE

Form Approved
OMB No. 0704-0188

1. AGENCY USE ONLY (Leave blank)	2. REPORT DATE	3. REPORT TYPE AND DATES COVERED
	April 1993	Final, June 1991–August 1992

4. TITLE AND SUBTITLE

Influence of Ply Waviness on Stiffness and Strength Reduction of Composite Laminates

5. FUNDING NUMBERS

PR: 1L162618AH80

6. AUTHOR(S)

Travis A. Bogetti, Jack W. Gillespie, Jr[1]., and Mark A. Lamontia[2]

7. PERFORMING ORGANIZATION NAME(S) AND ADDRESS(ES)

8. PERFORMING ORGANIZATION REPORT NUMBER

9. SPONSORING/MONITORING AGENCY NAME(S) AND ADDRESS(ES)

U.S. Army Research Laboratory
ATTN: AMSRL-OP-CI-B (Tech Lib)
Aberdeen Proving Ground, MD 21005-5066

10. SPONSORING/MONITORING AGENCY REPORT NUMBER

ARL-TR-110

11. SUPPLEMENTARY NOTES [1]Center for Composite Materials, Univ. of Delaware, Newark, DE. [2]E. I. DuPont De Nemours and Co., Inc., Engineering Technology Laboratory, Wilmington, DE. This work was sponsored by the Defense Advanced Research Projects Agency (DARPA), Naval Technology Program, under contract No. MDA972-89-C-0043. The work was performed at the University of Delaware's Center for Composite Materials located in Newark, DE.

12a. DISTRIBUTION/AVAILABILITY STATEMENT

Approved for public release; distribution is unlimited.

12b. DISTRIBUTION CODE

13. ABSTRACT *(Maximum 200 words)*

An analytic model is developed to investigate the influence of ply waviness on the stiffness and strength of composite laminates. The model predicts

- elastic properties and thermal expansion coefficients of sublaminates containing wavy layers
- ply stresses for prescribed mechanical and thermal load cases
- strength reduction associated with ply waviness

Parametric studies are conducted for sublaminates of AS4 Graphite/PEKK and S2 Glass/PEKK which exhibit layer waviness. Results show that stiffness and strength reduction are significant in the direction of ply undulation only. Mechanisms of stiffness reduction are attributed to out-of-plane rotation of wavy layers. This waviness may also create significant interlaminar shear stress that reduces strength. The magnitude of the property reduction increases as the amplitude of the undulation increases and the half-wavelength of the undulation decreases. Ply waviness represents one mechanism that may partially explain why the design and failure analyses of composite structures based on flat, autoclave cured coupon property data (minimal waviness), do not correlate well with test results.

14. SUBJECT TERMS

Ply waviness; strength (mechanics); thermoelastic properties; filament winding; thermoplastic composites; models; composite materials

15. NUMBER OF PAGES

46

16. PRICE CODE

17. SECURITY CLASSIFICATION OF REPORT	18. SECURITY CLASSIFICATION OF THIS PAGE	19. SECURITY CLASSIFICATION OF ABSTRACT	20. LIMITATION OF ABSTRACT
UNCLASSIFIED	UNCLASSIFIED	UNCLASSIFIED	UL

INTENTIONALLY LEFT BLANK.

TABLE OF CONTENTS

INTENTIONALLY LEFT BLANK.

LIST OF FIGURES

INTENTIONALLY LEFT BLANK.

LIST OF TABLES

INTENTIONALLY LEFT BLANK.

ACKNOWLEDGMENTS

This work was sponsored by the Defense Advanced Research Projects Agency (DARPA), Naval Technology Program, under contract No. MDA972-89-C-0043. The work was performed at the University of Delaware's Center for Composite Materials located in Newark, Delaware.

INTENTIONALLY LEFT BLANK.

1. INTRODUCTION

1.1 Manufacturing Issues and Ply Waviness. The quality and in-service performance of composite structures is strongly influenced by the manufacturing process. From autoclave curing of flat panel laminates to injection molding, the manufacturing process will inevitably influence the performance of the finished component. Quite often, "manufacturing defects" cannot be entirely eliminated and, therefore, must be tolerated. When designing composite structures, it is important to have a thorough understanding of the influence typical manufacturing defects can have on performance.

A frequently encountered manufacturing defect found in thick-section composite structures is ply waviness. Ply waviness is shown schematically in Figure 1 and represents a perturbation in ply orientation from the ideal case. The manufacture of composite cylinders, for example, is generally performed with the filament winding process where impregnated fiber bundles or tows are wound onto a mandrel of the desired shape. Ideally, fiber placement of the tows is such that they conform to the mandrel surface in the circumferential, axial, or some desired off-axis orientation. Undulation of the individual plies or tows may result from the manufacturing process. Ply waviness can significantly influence the performance of the cylinder by reducing its stiffness and strength.

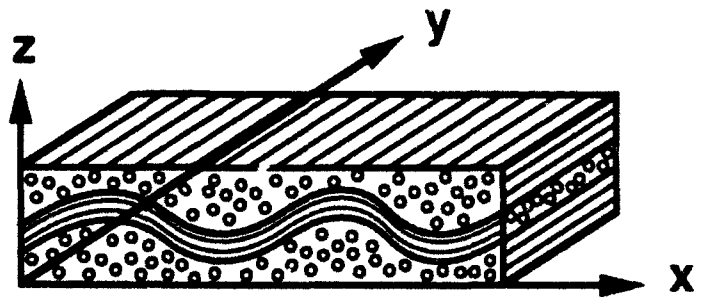

Figure 1. Ply Waviness in a Filament Wound Composite.

Currently, the manufacture of thermosetting composite cylinders is accomplished by first winding the entire cylinder followed by a post-curing and consolidation process. This process results in ply waviness through the thickness of the cylinder in both axially and circumferentially oriented plies. In contrast, filament-wound, thermoplastic, thick-walled cylinders can be manufactured with an "on-line" consolidation process, reducing ply waviness in the circumferential direction.

The effects of ply waviness in composite cylinders (or composite structures in general) can be studied by considering the effects of ply waviness in typical sublaminate (i.e., flat) configurations. Such an approach has been adopted in this work where a generic [90/0/90] sublaminate construction with a wavy [0] ply is investigated. In this report, an analytic model is developed to investigate the influence of ply waviness on the stiffness and strength of composite laminates. The model predicts:

- elastic properties and thermal expansion coefficients as a function of the constituent material properties and degree of undulation (ply waviness)

- individual ply stresses for prescribed mechanical and thermal load cases

- the strength reduction associated with ply waviness.

Parametric studies are presented which quantify the synergistic effects of ply waviness on stiffness and strength.

The theory developed in this work represents a useful design tool from which important manufacturing and design trade-offs can be made. The results presented indicate that the degree of waviness can significantly reduce the stiffness and strength of the structure.

The capabilities developed in this work for predicting the reduction in stiffness and strength due to ply waviness also represent a valuable tool for optimum structural design. For example, the reduced stiffness properties predicted can be employed as input into a suitable global stress analysis, resulting in a more realistic effective response prediction of the structural response as compared to a "defect free" analysis. The resulting stress fields predicted in the structure could then be used in conjunction with the failure analysis developed in this work to predict the reduction in strength associated with ply waviness. This design methodology ultimately results in a more realistic prediction of strength reduction due to ply

waviness, and provides valuable insight, in a consistent manner, into the dominant failure mechanisms characteristic of thick-section composite structures. The analytic model also provides a means of quantifying the economic trade-offs that exist between process refinement and material performance.

1.2 Literature Survey. The effects of the waviness of the ply layers on the mechanical performance of composite structures has received a considerable amount of attention in the published literature. The focus of relevant research has been on compression, since compression performance is known to be most influenced by waviness. In general, waviness in composites has been studied on two different levels: fiber waviness on the fiber/matrix level with individual fibers embedded in a surrounding matrix (i.e., in a single ply or lamina), and layer waviness of a complete ply or plies within a multidirectional laminate. An extensive literature review on waviness in composites is presented by Adams and Hyer (1992). A brief summary of the related research, however, is provided below for completeness.

The following literature is related to fiber waviness on the fiber/matrix level. Davis (1975) modeled fiber waviness in boron/aluminum composites using the classic microbuckling model (of straight fibers embedded in an elastic matrix) developed by Rosen (1965). Davis modeled the fibers as sinusoidal in shape and found shear bucking failure to be responsible for significant reductions in compression strength. A similar model was developed by Hyer (1986) who found that compression strength of wavy fibers decreased significantly with decreasing matrix shear modulus. In addition, he found the nonlinearity of the matrix material causes a further reduction in compression strength. Fiber kinking failure is closely related to fiber waviness. Consequently, numerous investigations have been conducted on the kinking failure of initially misaligned fibers (Argon 1972; Budiansky 1983; Steif 1990a, 1990b; Martinez et al. 1981).

The influence of fiber waviness on the effective elastic mechanical properties of composite lamina was investigated by Jortner (1984). The paper also provides a thorough review of the literature in this area. Jortner discusses the typical bounding techniques often employed in predicting the influence of fiber waviness on the effective elastic properties of composites. He presents an exact solution for predicting the elastic and thermal constants of wrinkled regions in composites; however, the model is limited to waviness that exhibits undulation which is completely in phase with the surrounding material.

More recently, investigators have began studying the effects of ply waviness in multidirectional laminates. These studies have focused on the interactions within and between adjacent plies within a laminate as opposed to interactions between individual fibers and the matrix material. Shuart (1985) studied the behavior of multidirectional laminates in uniaxial compression employing a microbuckling model. His models included a linear buckling analysis for short wavelength bucking and a geometrically nonlinear analysis for wavy layers. He observed that interlaminar shear stresses were a maximum at a point in the wavy ply where the out-of-plane undulation is greatest (i.e., the point of inflection). In addition, he concluded that laminate failure was caused by either short-wavelength bucking, interlaminar shear, or in-plane shear failures, depending on ply orientations and the degree of waviness. Total laminate compression strength reductions of up to 36% were reported. Shuart (1989) subsequently included a matrix compression failure mode and in-plane ply waviness in his analysis. His work was further extended by Peel (1990) who considered additional failure modes as well as a variety of wavy ply geometries and configurations.

Hyer, Maas, and Fuchs (1988) and Telegadas and Hyer (1990) have studied the effects of ply waviness on the stress states in hydrostatically loaded cylinders. They employed finite element analyses to study the influence the geometry of the waviness and material properties on the stress states that develop. They observed significant interlaminar stress levels in wavy plies and found material property variations to be important factors in the magnitude of stresses produced.

The influence of ply waviness on the performance of cylinders has also been investigated experimentally by Garala (1989). In this study, numerous 8-in monocoque graphite/epoxy cylinders were hydrostatically loaded to failure. Cylinder failures might have been initiated by interlaminar shear failure due to ply waviness in the hoop and axial directions.

The approach taken in this work follows closely that of Ishikawa and Chou (1982, 1983a, 1983b, 1983c) in their studies of the thermomechanical behavior of two-dimensional woven fabric composites. As with the models they developed, the theoretical basis for the model developed here is laminated plate theory. The success of their models for predicting the effective thermomechanical properties of woven fabric composites provides initial confidence in and a point of departure for the results generated in this work.

1.3 Problem Statement. The objective of this work is to quantify the influence of manufacturing induced ply waviness on the stiffness and strength in a composite and to assess the affect on structural performance. Ply waviness is assumed to exist in one direction only. A schematic illustrating ply waviness is shown in Figure 1, where the wavy ply is undulating in the x-direction. This layer is defined as a [0] ply which is embedded in [90] plies or lamina having straight fibers aligned in the y-direction.

The models developed in this work predict the in-plane (x-y plane) longitudinal modulus, E_x; transverse modulus, E_y; in-plane Poisson ratio and shear modulus, ν_{xy} and G_{xy}, respectively, as a function of the undulation geometry and material properties of the composite lamina. The in-plane thermal expansion coefficients, α_x and α_y, are also predicted.

In addition to the elastic properties, the model developed calculates the stresses in the [0] and [90] plies as a function of geometric location and effective in-plane plate loadings. The stresses in the [90] ply will be in-plane only, while out-of-plane stresses in the [0] ply will develop due to the inclination of the ply out of the x-y plane. The magnitude of the stress components in each ply will vary along the length of the undulation due to a constant in-plane stress resultant assumption. Once the stresses in the individual plies are calculated, the maximum stress failure criterion is applied to predict ultimate failure of the wavy ply configuration. The maximum stress failure criterion is chosen because it identifies the failure mode and provides the greatest physical insight into the mechanisms of strength reduction. With the failure analysis capability, the influence of waviness on strength reduction is quantified. Thermal, uniaxial, and biaxial loadings are also investigated.

2. ANALYSIS

2.1 Background: Laminated Plate Theory. The theoretical development of the analysis is presented in this section. The basis for the analytic model developed is laminated plate theory (Whitney, Daniel, and Pipes 1982; Whitney 1987). Laminated plate theory is well developed and, consequently, only equations pertinent to the analysis developed here are presented.

Laminate response is generally described through a relationship between effective plate loadings and plate deformation. Typically, the relationship between in-plane stress and moment resultants, N_i and M_i, and in-plane strains and curvatures, ε_i and κ_i, is given by

$$\begin{Bmatrix} N_i \\ M_i \end{Bmatrix} = \begin{bmatrix} A_{ij} & B_{ij} \\ B_{ij} & D_{ij} \end{bmatrix} \begin{Bmatrix} \varepsilon_j^o \\ \kappa_j \end{Bmatrix} \quad (i,j = 1,2,6) \tag{1}$$

where the A_{ij}, B_{ij}, and D_{ij} stiffness matrices are defined in the usual manner as

$$(A_{ij}, B_{ij}, D_{ij}) = \sum_{k=1}^{n} \int_{h_{k-1}}^{h_k} (1, z, z^2)\,(Q_{ij})^k\, dz \tag{2}$$

or simply

$$A_{ij} = \sum_{k=1}^{n} (Q_{ij})^k\,(h_k - h_{k-1})$$

$$B_{ij} = \sum_{k=1}^{n} (Q_{ij})^k\,\frac{1}{2}\,(h_k^2 - h_{k-1}^2)$$

$$D_{ij} = \sum_{k=1}^{n} (Q_{ij})^k\,\frac{1}{3}\,(h_k^3 - h_{k-1}^3)\,. \tag{3}$$

The lamina stiffness matrix for the k^{th} ply is $(Q_{ij})^k$, n is the total number of plies in the laminate, and h_k is the distance from the laminate midplane to the k^{th} ply surface. An alternative form of Equation 1 is obtained through its inversion and is given as

$$\begin{Bmatrix} \varepsilon_i^o \\ \kappa_i \end{Bmatrix} = \begin{bmatrix} a_{ij} & b_{ij} \\ b_{ij} & d_{ij} \end{bmatrix} \begin{Bmatrix} N_j \\ M_j \end{Bmatrix} \tag{4}$$

where a_{ij}, b_{ij}, and d_{ij} are the compliance matrices that describe the effective plate-like behavior of the laminate. These compliance components are the terms ultimately used to compute the effective in-plane thermomechanical properties of the laminate.

2.2 Description of the Geometry. In order to quantify the influence of ply waviness on stiffness and strength reduction, a mathematical description of the geometry is required. From the wavy ply configuration depicted in Figure 1, a unit cell is idealized and is shown in Figure 2. A half-sine wave segment of the undulation is selected as a representative element for the wavy ply configuration. The unit cell, having a total thickness h_t, consists of an unduling [0] ply with thickness h_f lying between two [90] regions. The amplitude of the undulation is A. The half-wavelength of the undulation is L. The [90] plies are aligned in the y-direction and are assumed to have no undulation.

Detailed mathematical descriptions of the individual plies within the unit cell expressed as a function of x are required. Referring to Figure 2, the following distances along the half-sine wave shaped undulation are defined by

$$
\begin{aligned}
h_1(x) &= -h_t/2 \\
h_2(x) &= -A/2 - h_f/2 + [1 + \sin(\frac{\pi}{L}(x - \frac{L}{2}))]\, A/2 \\
h_3(x) &= -A/2 + h_f/2 + [1 + \sin(\frac{\pi}{L}(x - \frac{L}{2}))]\, A/2 \\
h_4(x) &= h_t/2 \quad .
\end{aligned}
\tag{5}
$$

A local out-of-plane undulation angle, θ, is also needed. Referring to Figure 3, θ can be defined as a function of x as

$$
\theta(x) = \tan^{-1}\left[\frac{d(h_2(x))}{dx}\right] = \tan^{-1}\left[\frac{d(h_3(x))}{dx}\right] \quad . \tag{6}
$$

2.3 Effective Elastic Properties. The in-plane thermomechanical properties of the unit cell are representative of the response to be expected of the entire wavy ply. The approach taken here is to divide the unit cell into discrete segments of width dx in the direction of undulation (see Figure 3). The unit cell is defined by the thickness of the smallest repeating sublaminate employed during fabrication, h_t, as well as h_f, A, and L defined previously. A systematic, laminated plate theory analogy is applied to each segment. The effective response of the unit cell is obtained through an averaging approach where an

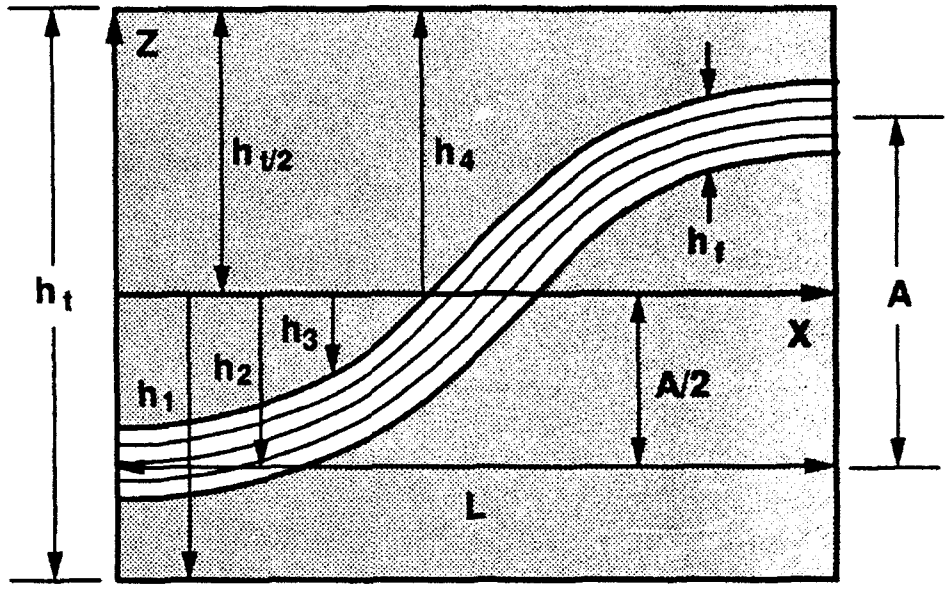

Figure 2. [90/0/90] Ply Waviness: Unit Cell.

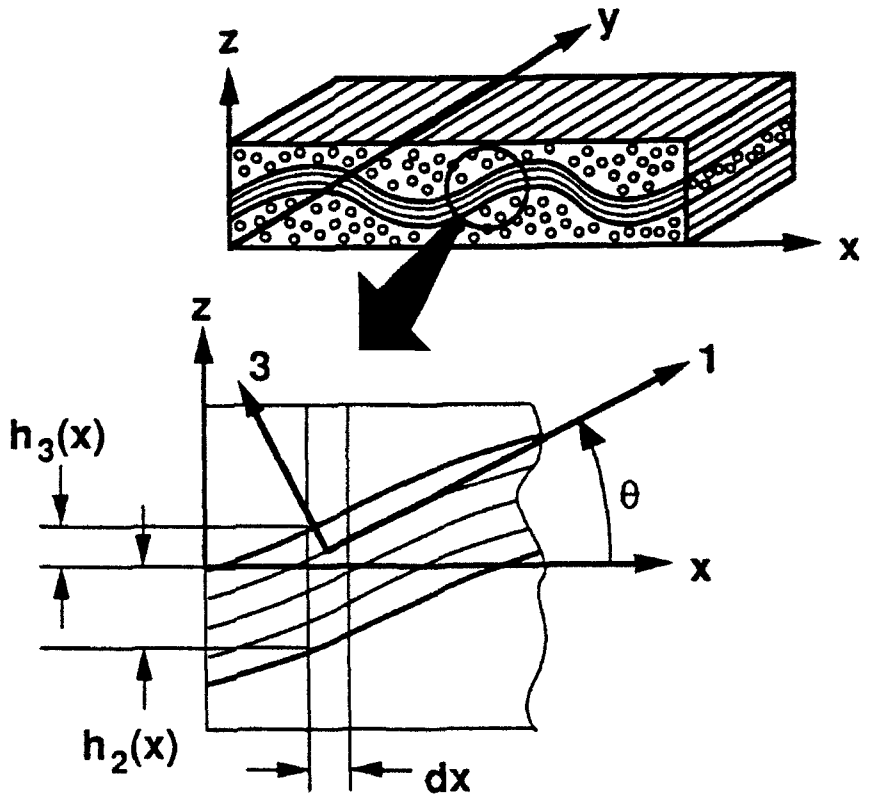

Figure 3. Laminate Analogy for [90/0/90] Ply Waviness.

in-plane stress resultant is assumed constant within each discrete segment. In this approach, average compliances are obtained through an integration procedure and subsequent calculations are made to evaluate the effective thermomechanical properties of the unit cell as a function of ply waviness.

The A_{ij}, B_{ij}, and D_{ij} stiffness matrices for each discrete segment of width dx within the unit cell are first computed through Equation 3 using the $h_i(x)$ values defined in Equation 5. The unit cell is essentially a three-ply laminate with x-dependent A_{ij}, B_{ij}, and D_{ij} stiffness matrices. The thickness of individual piles are defined by the [90/0/90] laminate stacking sequence to be investigated. The Q_{ij}'s for the [90] plies are constant along the x-direction and are computed from the typical engineering constants of the straight lamina (i.e., E_1, E_2, ν_{12}, and G_{12}) in the usual fashion (Whitney, Daniel, and Pipes 1982; Whitney 1987). The Q_{ij}'s for the [0] ply, however, must take into account the out-of-plane (z-direction) orientation. The effective engineering properties used to compute the Q_{ij}'s in each dx segment along the x-direction are a function of the inclination angle, θ, and are given by

$$
\begin{aligned}
E_x(\theta) &= [\, l_\theta^4 / E_1 + (1/G_{13} - 2\nu_{13}/E_1)\, l_\theta^2 m_\theta^2 + m_\theta^4 / E_3 \,]^{-1} \\
E_y(\theta) &= E_2 \\
\nu_{xy}(\theta) &= E_x(\theta)\left[\frac{l_\theta^2 \nu_{12}}{E_1} + \frac{\nu_{32} m_\theta^2}{E_3}\right] \\
G_{xy}(\theta) &= \left[\frac{m_\theta^2}{G_{23}} + \frac{l_\theta^2}{G_{12}}\right]^{-1} \\
l_\theta &= cos\theta \\
m_\theta &= sin\theta
\end{aligned}
\tag{7}
$$

where E_1, E_2, G_{12}, ν_{12}, and G_{23} are the typical principal system engineering constants of the straight lamina. The effective a_{ij}, b_{ij}, and d_{ij} compliance matrices for each dx segment within the unit cell are computed through inversion of the A_{ij}, B_{ij}, and D_{ij} stiffness matrices according to Equation 4.

The local warping constraint is imposed on each dx segment in the unit cell. This assumption leads to a more realistic estimate of the effective response of the wavy ply configuration since no global out-of-plane warping is expected in an axisymmetric geometry or in a laminate of appreciable thickness.

Under the local warping constraint, a zero curvature and non-zero moment condition are imposed. The bending free or local warping constraint behavior of each dx segment can be expressed as a function of the full a_{ij}, b_{ij}, and d_{ij} compliance matrices defined in Equation 4 (Ishikawa and Chou 1983a),

$$a_{ij}^{*} = [a_{ij} - b_{ij}\, d_{ij}^{-1}\, b_{ij}] \quad , \tag{8}$$

where a_{ij}^{*} is now the in-plane compliance matrix with local warping constrained.

In order to calculate the average or effective response of the wavy ply, an average in-plane compliance matrix is defined. Assuming a uniform in-plane stress resultant exists in each dx segment, the average in-plane compliance matrix is obtained through the following integration over the entire unit cell length:

$$a_{ij}^{**} = \frac{1}{L} \int_0^L a_{ij}^{*}(x)\, dx \quad . \tag{9}$$

Here a_{ij}^{**} is the effective in-plane compliance matrix for the wavy ply with the local warping condition imposed. Similarly, the compliance matrices b_{ij} and d_{ij} could be defined, however, these matrices are not employed in determining the effective in-plane mechanical properties of the wavy ply construction (see Equation 8).

The effective in-plane mechanical properties of the wavy ply are computed from the following a_{ij}^{**} compliance coefficients according to

$$\begin{aligned} E_x &= \frac{1}{h_t\, a_{11}^{**}} \\ E_y &= \frac{1}{h_t\, a_{22}^{**}} \\ \nu_{xy} &= \frac{-a_{12}^{**}}{a_{11}^{**}} \\ G_{xy} &= \frac{1}{a_{33}^{**}} \quad . \end{aligned} \tag{10}$$

It is noted that the effective in-plane mechanical properties with local warping allowed could have been computed in a more straightforward fashion than those computed with the local warping constrained condition applied. The procedure is essentially identical to that outlined above with the step taken in Equation 8 omitted. This procedure would predict stiffnesses significantly more compliant due to unconstrained warping of the unit cell.

2.4 Effective Thermal Expansion Coefficients. A similar approach for the prediction of the effective mechanical properties of the wavy ply construction is taken in calculating the effective thermal expansion coefficients. In-plane thermal load resultants, N_j^{th}, in each dx segment of the unit cell are required and are computed through the following equation:

$$N_j^{th} = \sum_{k=1}^{n} \int_{h_{k-1}}^{h_k} (Q_{ij})^k (h_k - h_{k-1}) \alpha_j^k \Delta T \, dz \quad , \tag{11}$$

where ΔT is the uniform thermal load, and the α_j's are the in-plane thermal expansion coefficients of the [0] and [90] plies. Here again both Q_{ij} and α_j in the [90] ply are constant along the x-direction within the unit cell. The [0] ply properties are functions of $\theta(x)$ (Equation 6) and are transformed into the x-y coordinate system from the principal coordinate system defined by the local fiber orientation shown in Figure 3. Thermal expansion coefficients for each segment are defined by

$$\left\{\alpha_i^*\right\} = \left[a_{ij}^*\right] \left\{N_j\right\}^{th} \tag{12}$$

where a_{ij}^* is that computed in Equation 8. The effective in-plane thermal expansion coefficients for the wavy ply configuration, α_i^{**} are then calculated by the same averaging approach described above through

$$\alpha_i^{**} = \frac{1}{L} \int_0^L \alpha_i^* (x) \, dx \quad . \tag{13}$$

This completes the theoretical development of the analytic model for predicting the effective thermomechanical properties of the wavy ply configuration. In the following section, the determination of the individual [0] and [90] ply stresses and strength analysis are discussed.

2.5 Ply Stresses. In order to gain a fundamental understanding of the failure mechanisms associated with wavy plies and to quantify the influence of the degree of undulation on strength reduction, individual ply stresses in the wavy ply configuration must be computed. Individual ply stresses in both the [0] and

[90] plies are computed from given or defined in-plane stress resultants in the x- and y-directions (Figure 1). Recalling that a constant in-plane stress resultant within the unit cell was assumed, the individual ply stresses are expected to vary along the x-direction within the unit cell due to the undulating [0] ply. The procedure for computing these stresses is outlined below.

For a given set of in-plane stress resultants due to thermal or mechanical loading, N_j, the in-plane strains within each dx segment within the cell are computed by

$$\left\{\varepsilon_i^*\right\} = \left[a_{ij}^*\right]\left\{N_j\right\} \tag{14}$$

where a_{ij}^* is the compliance matrix computed in Equation 8. It should be understood that the in-plane strains (defined in the x- and y-directions) of each ply within a single dx segment are identical through the thickness (z-direction) but vary along the length (x-direction). Since local warping is constrained, the in-plane strains represent the total ply strains and the typical strain displacement relation is not required. The individual ply stresses (in the x- and y-directions) within each dx segment are evaluated through Hooke's law relation given by

$$\left\{(\sigma_i^*)^k\right\} = \left[(Q_{ij})^k\right]\left\{(\varepsilon_j^*)^k - (\alpha_j)^k \Delta T\right\} \tag{15}$$

where the Q_{ij}'s are the same as those used in the effective mechanical property calculations.

While Equation 15 provides the ply stresses in each dx segment defined in the global x- and y-directions, these stresses must be transformed into the principal system of the [0] and [90] plies. The principal material coordinate system for a unidirectional lamina is shown in Figure 4. Referring to Figures 1 and 4, the longitudinal or 1-direction stresses in the [90] plies will correspond to y-direction stresses calculated in Equation 15. Transverse or 2-direction stresses in the [90] plies will correspond to the calculated x-direction stresses.

Referring to Figures 1 and 4, the 2-direction stresses in each dx segment of the [0] ply correspond to the calculated y-direction stresses. The situation is slightly more complicated, however, for computing the other principal stress components in the [0] ply. Since the [0] ply is undulating out of the x-y plane, transverse normal (3-direction) and interlaminar shear stress (1-3) components will develop within the unit

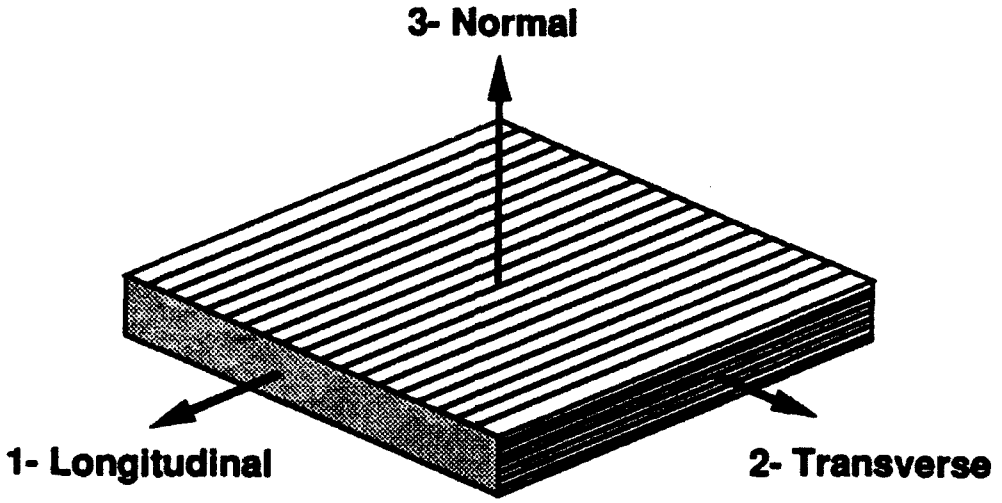

Figure 4. Lamina Coordinate System.

cell. These stress components result solely from the x-direction stresses and are computed through tensoral transformation of the x-direction stress components.

In summary, the [90] plies will contain 1- and 2-direction stress components only. The [0] ply will contain 1, 2, 3 and 1-3 stress components due to the out-of-plane undulation within the unit cell. Furthermore, these stress components will vary along the x-direction within the unit cell. Understanding these stress variations will provide fundamental insight into the dominant failure mechanisms characteristic of wavy plies. In the next section, the failure criterion applied to the wavy ply configuration is presented.

2.6 Applied Failure Criterion: Maximum Stress. The failure analysis developed in this investigation is based on the maximum stress failure criterion. Failure of the wavy ply configuration is defined when a principal stress component in either the [0] or [90] plies of any dx segment along the unit cell reaches its corresponding strength allowable. To provide results that are useful in making design decisions based on the failure analysis, a scaling approach which determines the effective in-plane load resultants at failure was adopted. For a given wavy ply geometry configuration, the in-plane load resultants for each dx element along the unit cell which would initiate failure are computed. The lowest load resultant for any

segment over the entire length of the unit cell defines the loads at failure for the entire wavy ply configuration. Strength reduction associated with ply waviness is based on comparisons between failure loads of the wavy ply configuration to those of a similar straight laminate configuration having zero amplitude of undulation.

Both in-plane mechanical loading and thermal loading have been incorporated into the analysis. Thermal loading is applied in the form of a uniform temperature differential. Thermal loads at failure are scaled in the same manner described above. In addition, a combination of thermal and mechanical loading as well as biaxial loading are permitted.

3. RESULTS

Parametric studies illustrating the results from the analytical models developed above for predicting the thermomechanical properties, ply stresses, and strength reduction in wavy plies are presented in this section. Significant findings are reported in the body of this report while less interesting results generated have been documented in the Appendix. Before the results are presented, a constraint on the geometric parameters describing the wavy ply configuration is discussed. Results are generated for both AS4-Carbon/PEKK and S2-Glass/PEKK composite material systems. A summary of the geometric parameters, material properties, and strength allowable used in the parametric studies is presented.

3.1 Geometric Constraint on Ply Waviness. To describe the physical geometry of the wavy ply configuration, a parameter that identifies the ratio of the total [90] ply thickness (t_{90}) to [0] ply thickness (t_0), TR (thickness ratio), is required

$$TR = \frac{2 \cdot t_{90}}{t_0} = \frac{2 \cdot t_{90}}{h_f} \quad . \tag{16}$$

The definition of this ratio is illustrated in Figure 5. Once a TR ratio is defined, the total thickness of the unit cell becomes

$$h_t = h_f(1 + TR) \tag{17}$$

A geometric constraint imposed on the amplitude of the [0] ply undulation wavy ply configuration for a given h_t and h_f is identified in Figure 6 to be

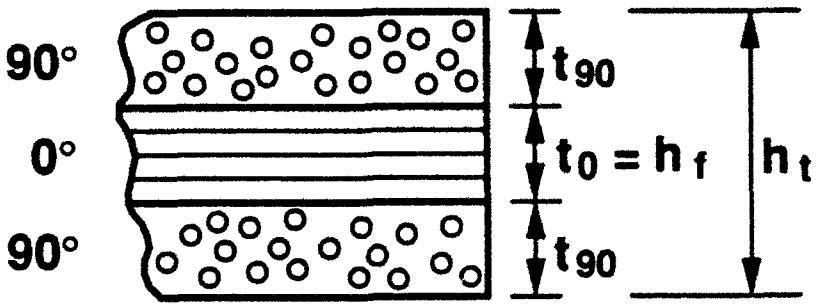

Figure 5. Definition of Thickness Ratio: *TR*.

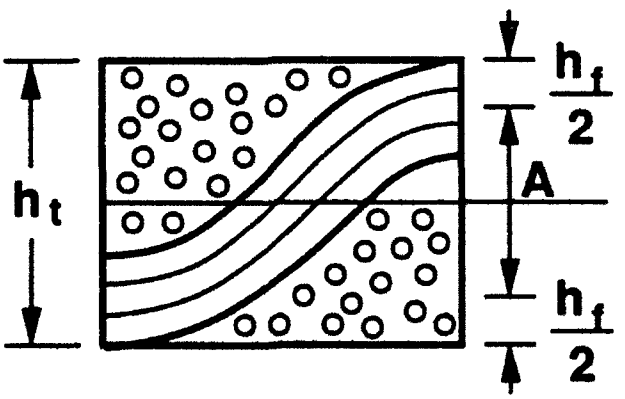

Figure 6. Geometric Constraint on Amplitude.

$$A < h_t - h_f \quad . \tag{18}$$

In the remainder of this section, parametric studies are presented to illustrate the significant findings of this work. Presentation of the results is facilitated with the comprehensive illustration indicating all details of the wavy ply configuration including the global and ply coordinate systems used in the analysis (see Figure 7).

3.2 Parametric Studies. Parametric studies were conducted between zero amplitude and the value defined in Equation 18 to bound the potential process-induced reduction in stiffness and strength. Photomicrographs of actual filament wound composite cylinders, however, revealed that the nominal amplitudes were much less than this upper bound. Photomicrographs were useful in defining a range of half-wavelengths to be investigated in this study. The most common wavelength observed was approximately 20 ply thicknesses, h_f, which correlated well with the nominal width of the tow employed during filament winding. The geometric parameters studied are listed in Table 1. A constant [0] ply thickness of 0.005 inches was used as the baseline. Tables 2 and 3 summarize the experimentally determined mechanical properties and strength allowables of the AS4 Carbon/PEKK and S2 Glass/PEKK composite systems used in the study.

3.2.1 Effective Elastic Properties. The influence of various geometric parameters on the effective elastic properties of the wavy ply configuration were investigated first. The influence of undulation amplitude, A, on the reduction of x-direction modulus, E_x, for the AS4 Graphite/PEKK composite is shown in Figure 8 for various TR ratios and a unit cell length of $L = 5 \cdot h_f$. Stiffness reduction is defined as the ratio of wavy ply stiffness to the stiffness of an equivalent laminate construction with a zero undulation amplitude. The results indicate significant stiffness reduction of up to 60% for A/h_f values below 5 in this extreme case. The influence of increasing the unit cell length to $L = 20 \cdot h_f$ is shown in Figure 9. Stiffness reduction was not as severe (<30%) for A/h_f values below 5. The same study for a unit cell length of $L = 5 \cdot h_f$ for the S2 Glass/PEKK composite is shown in Figure 10. This study indicates that stiffness reductions in the glass system are not as sensitive to undulation amplitude as in the carbon system. This is true because the graphite system exhibits substantially more anisotrophy in the fiber direction than the glass composite. Other in-plane mechanical properties such as transverse stiffness, E_y, poisson ratio, ν_{xy},

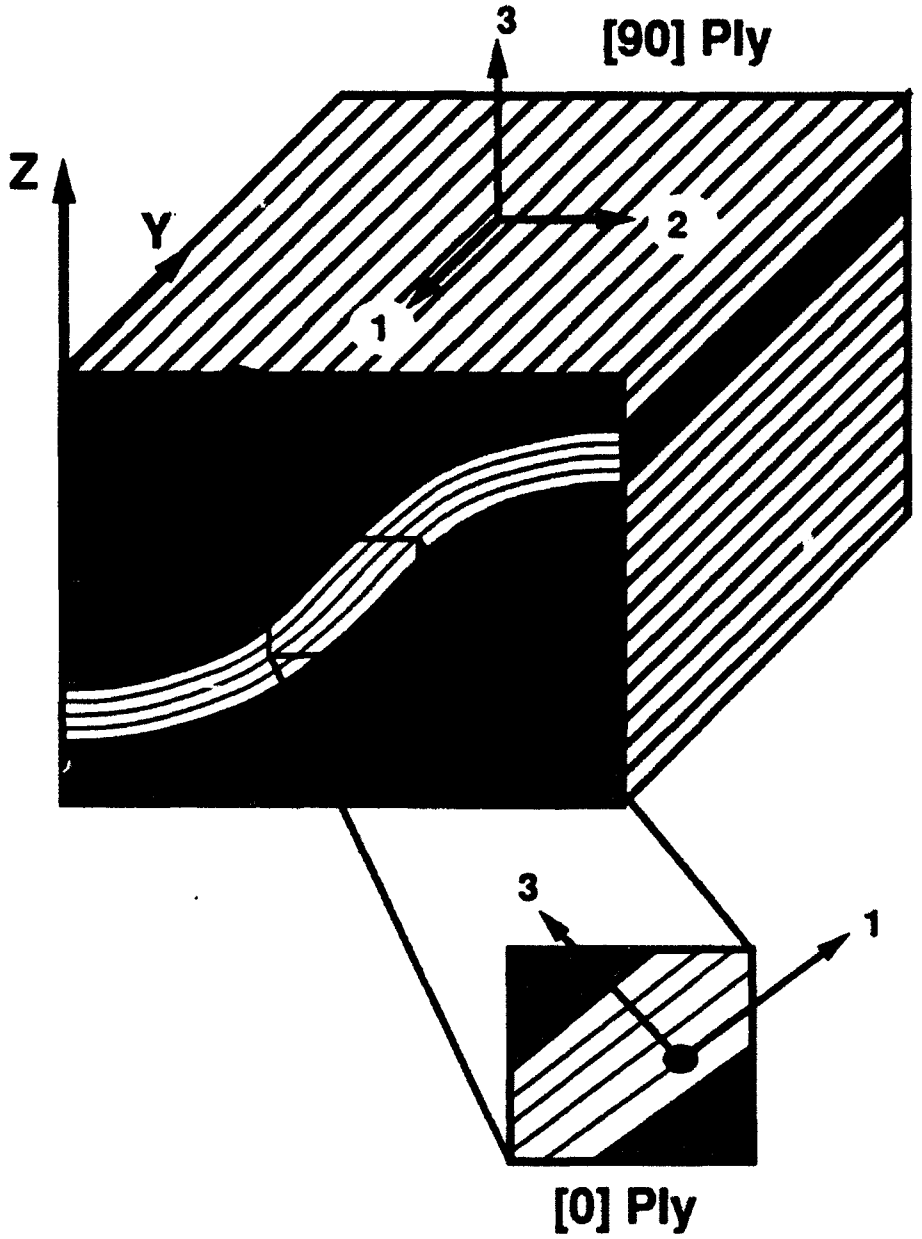

Figure 7. Global and Ply Coordinate Systems Used in Analysis.

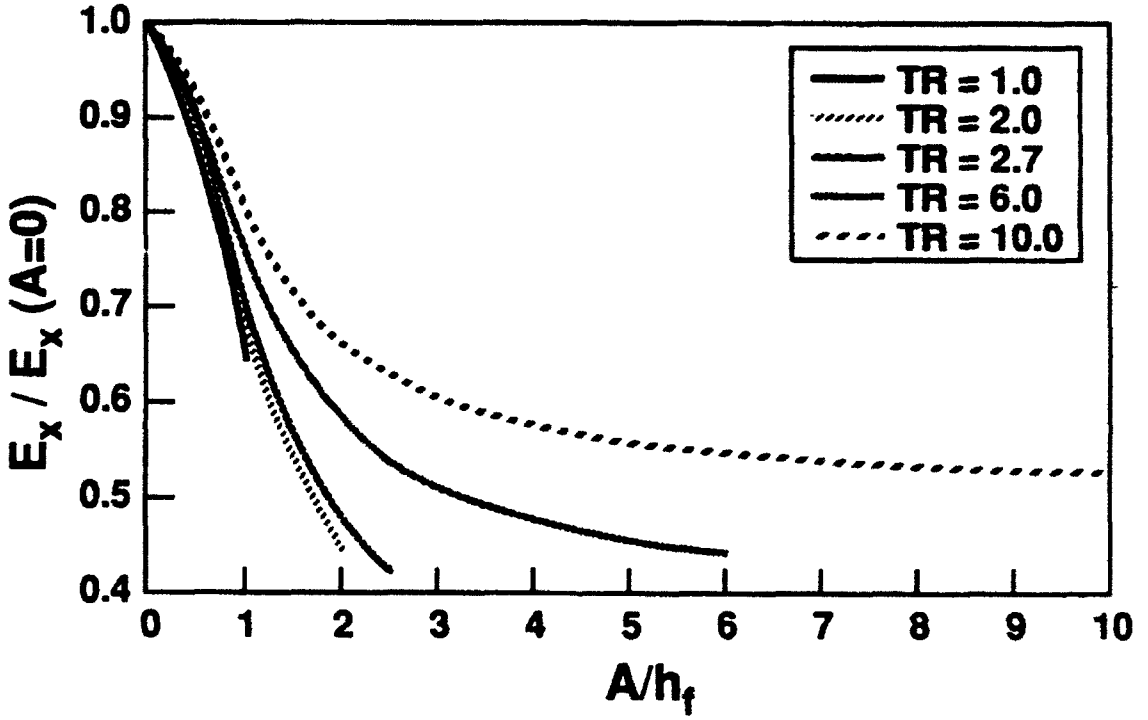

Figure 8. Influence of Undulation Amplitude on E_x in AS4 Graphite/PEKK ($L/h_f = 5$).

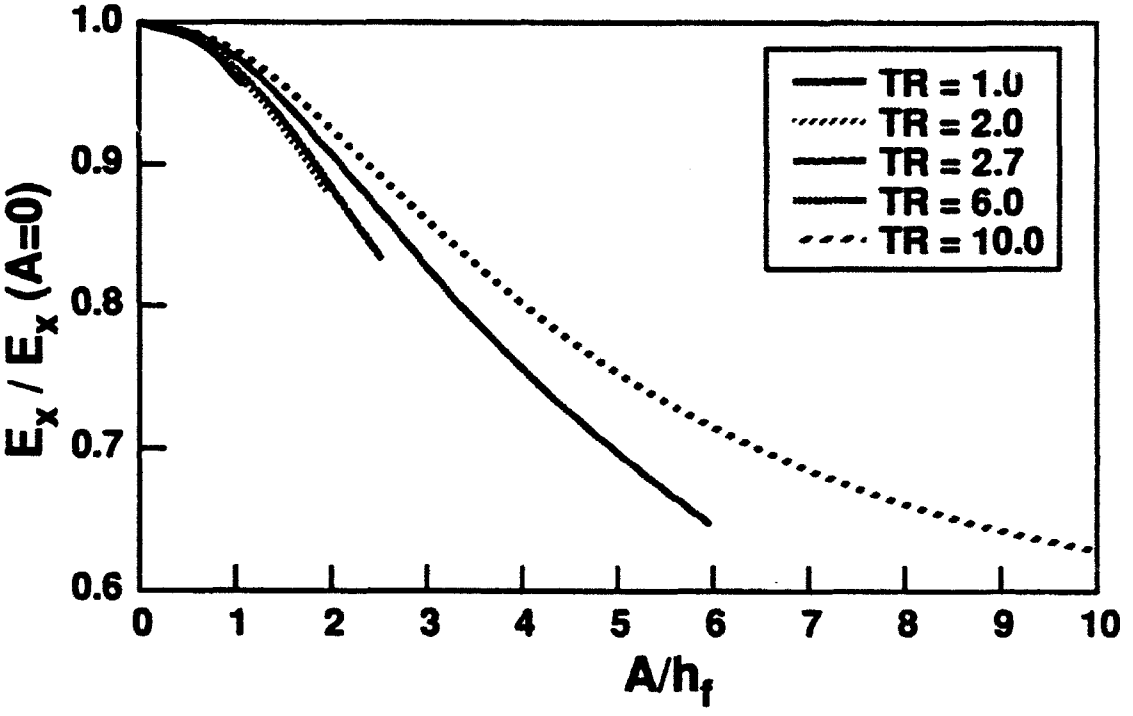

Figure 9. Influence of Undulation Amplitude on E_x in AS4 Graphite/PEKK ($L/h_f = 20$).

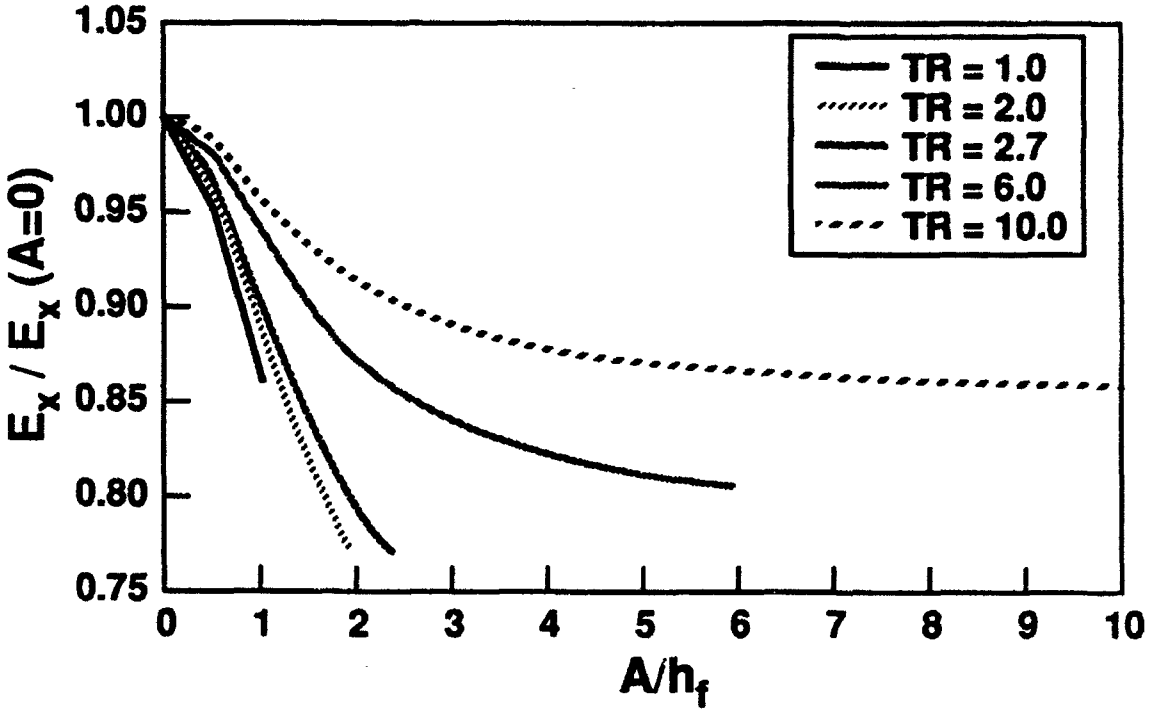

Figure 10. Influence of Undulation Amplitude on E_x in S2 Glass/PEKK ($L/h_f = 5$).

Table 1. Parameter Study: Geometry

TR	h_t (in)	A_{max} (in)
1.0	0.010	0.005
2.0	0.015	0.010
2.7	0.0185	0.0135
6.0	0.035	0.03
10.0	0.055	0.05
$\frac{L}{h_f} = 5, 20, 50$		

Table 2. Material Properties

Property	AS4 Graphite/PEKK	S2 Glass/PEKK
E_1 (Msi)	17.0	8.0
E_2 (Msi)	1.40	2.75
G_{12} (Msi)	0.98	1.01
G_{23} (Msi)	0.98	0.59
ν_{12}	0.36	0.27
ν_{23}	0.36	0.31
α_1 (με/°F)	–0.5	2.3
α_2 (με/°F)	15.5	18.5
α_3 (με/°F)	15.5	18.5

Table 3. Strength Allowables

Allowable	AS4 Graphite/PEKK	S2 Glass/PEKK
$X1T$ (ksi)	285	243
$X2T$ (ksi)	5.2	7.0
$X3T$ (ksi)	5.2	8.5
$X1C$ (ksi)	155	177
$X2C$ (ksi)	26.5	30.6
$X3C$ (ksi)	26.5	35.0
$S13$ (ksi)	15.2	17.0
$S12$ (ksi)	19.0	15.7

in-plane shear modulus, G_{xy}, were found to be relatively insensitive to undulation amplitude in the x-direction for both material systems studied (see Appendix A).

In general, stiffness reduction is most severe in the carbon system, increasing with increasing undulation amplitude and decreasing unit cell length.

3.2.2 Effective Thermal Expansion Coefficients. Increasing undulation amplitude was found to increase the x-direction thermal expansion coefficient up to 70% in the carbon system with $L = 20 \cdot h_f$ (Figure 11). A 30% increase in the glass system is predicted for $L = 5 \cdot h_f$ (Figure 12). The increase is associated with the out-of-plane rotation of the axial plies which decreases axial stiffness and provides less constraint on thermal deformation of the [90] plies. Changes in transverse thermal expansion were found to be insignificant in all cases investigated (see Appendix A).

3.3 Ply Stresses. Ply stresses along the unit cell length predicted from the analysis are presented to provide insight into the dominant failure mechanisms characteristic of the wavy ply configuration. Ply stresses are nondimensionalized by the corresponding strength allowables presented for the AS4 Graphite/PEKK composite system in Table 3. The magnitude of the ply stresses are calculated from a uniaxial x-direction load resultant that would cause failure of an identical laminate, except with a zero amplitude wavy ply configuration (N_x = 901 lb/in). Ply stresses in the [0] layer in the principal 1-direction are presented in Figure 13 for undulation amplitudes $A \leq 0.01$ in. Stress components are shown to be a

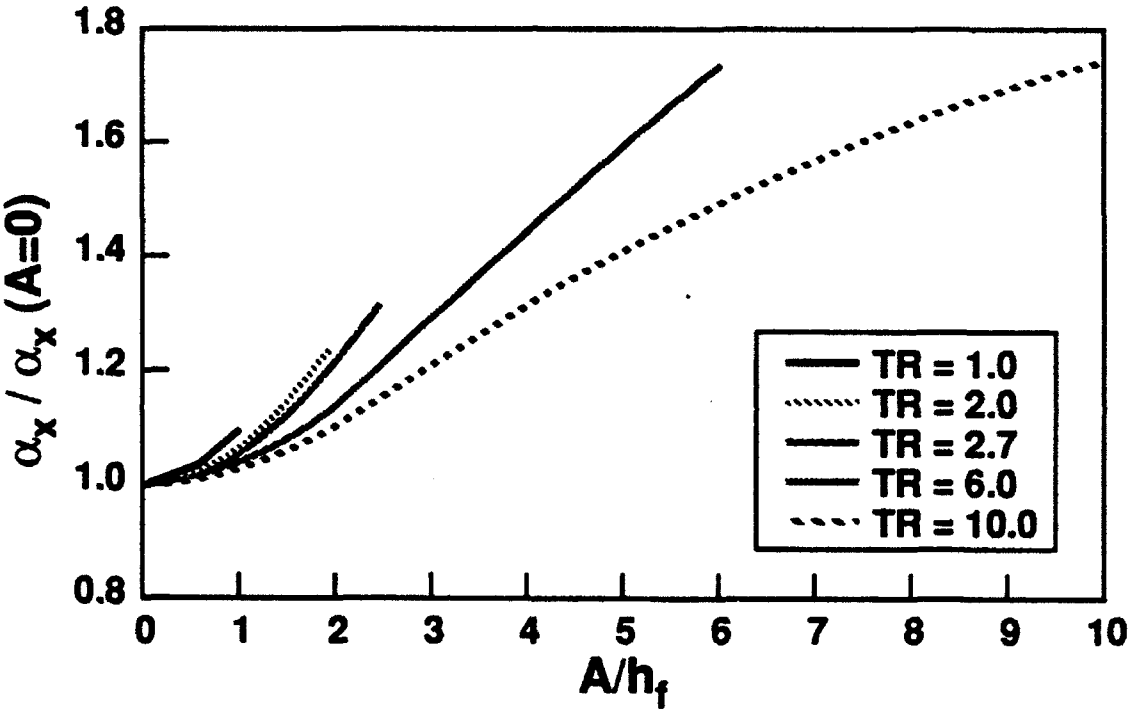

Figure 11. Influence of Undulation Amplitude on α_x in AS4 Graphite/PEKK ($L/h_f = 20$).

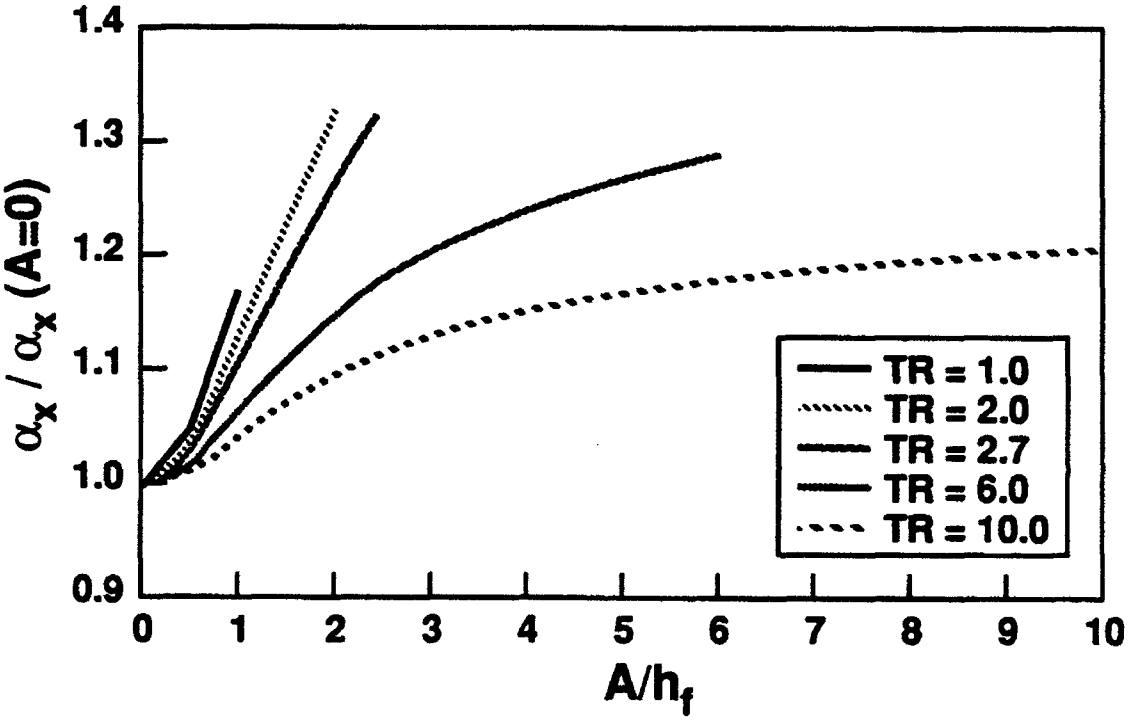

Figure 12. Influence of Undulation Amplitude on α_x in S2 Glass/PEKK ($L/h_f = 5$).

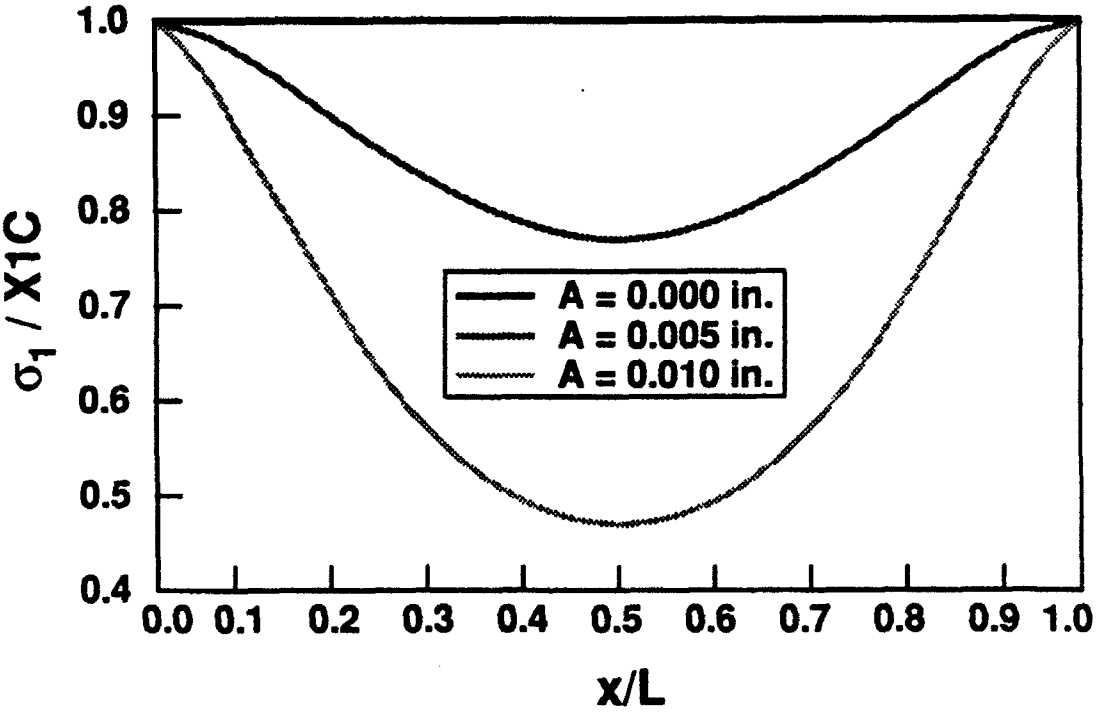

Figure 13. Longitudinal Stress Within a Wavy [0] Ply in AS4 Graphite/PEKK: Uniaxial Loading ($TR = 2$, $L/h_f = 5$, N_x ($A = 0$) = –901 lb/in at Failure).

minimum in regions within the unit cell where out-of-plane orientations are maximum. In this situation, the load is transferred to the 2-direction of the [90] plies to satisfy force equilibrium.

Interlaminar normal (3-direction) and shear stress components (1-3) in the [0] ply are shown in Figures 14 and 15 for the same load situation. Normal stress components are significant in the region of maximum undulation, reaching just beyond the strength allowable in this example. The interlaminar shear stress components, however, are far more significant reaching nearly three times the strength allowable for this extreme case. Other less significant results, including [90] ply stress plots and load cases in the *y*-direction, are documented in Appendix B.

The most significant finding of the parametric study is the high interlaminar shear stress components that develop in the [0] plies due to the out-of-plane orientation. The stress levels observed indicate that this is a dominant failure mode when the wavy ply configuration is loaded in the direction of undulation. It also quantifies the influence of undulation amplitude on the ply stress levels that develop and demonstrates the importance of controlling ply waviness in the load direction during manufacture. These observations are also consistent with those made by Hyer, Maas, and Fuchs (1988) and Telegadas and Hyer (1990).

3.4 Strength Reduction Due to Ply Waviness.

3.4.1 Uniaxial Loading. Clearer insight into the influence of ply waviness on strength reduction is achieved by examining the reduction in the ultimate applied load resultant that the wavy ply configuration can withstand before the stress component in any ply reaches its corresponding strength allowable. In Figures 16 and 17, strength reduction in AS4 Graphite/PEKK wavy ply configurations of ($A \leq 0.01$ in) length $L = 5 \cdot h_f$ and $20 \cdot h_f$ are presented for a uniaxial loading in the *x*-direction. These results indicate that significant strength reduction (65% for $L = 5 \cdot h_f$ and 35% for $L = 20 \cdot h_f$) along the unit cell length is possible. It is pointed out that the dominant failure mode transitions from a longitudinal compressive failure (*X1C*) in the [0] ply to interlaminar shear failure (*S13*) in the [0] ply in regions where the out-of-plane orientation increases. Other results show that ply waviness in the *x*-direction does not significantly affect the *y*-direction strength allowable.

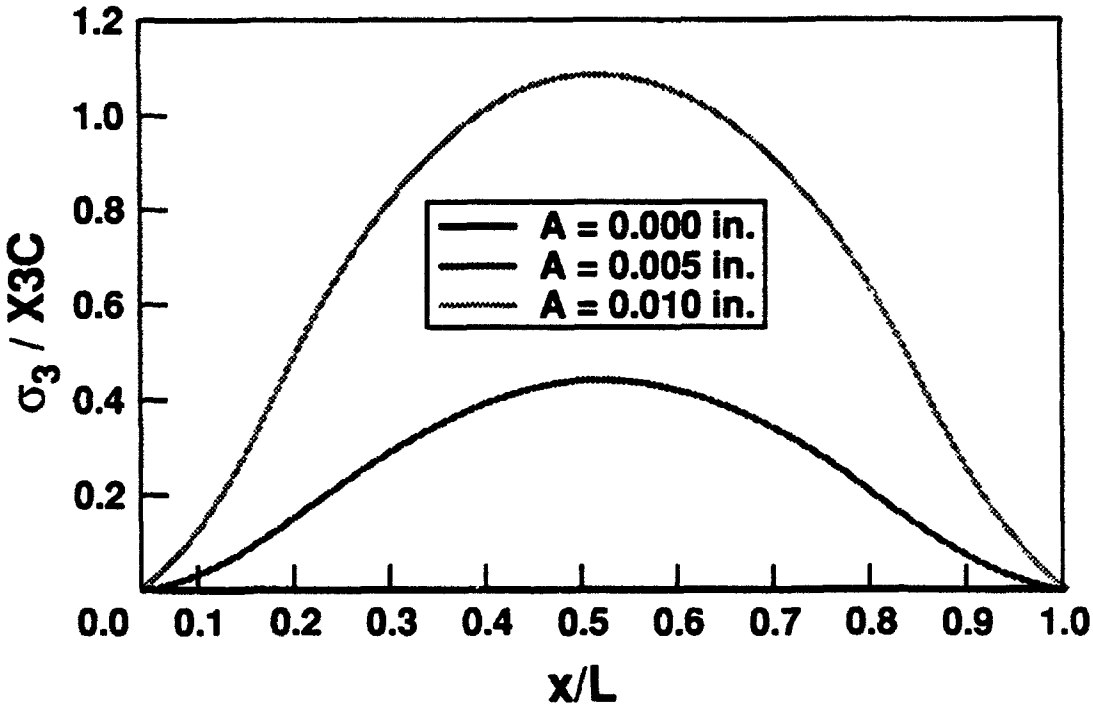

Figure 14. Interlaminar Normal Stress Within a Wavy [0] Ply in AS4 Graphite/PEKK: Uniaxial Loading ($TR = 2$, $L/h_f = 5$, N_x ($A = 0$) = –901 lb/in at Failure).

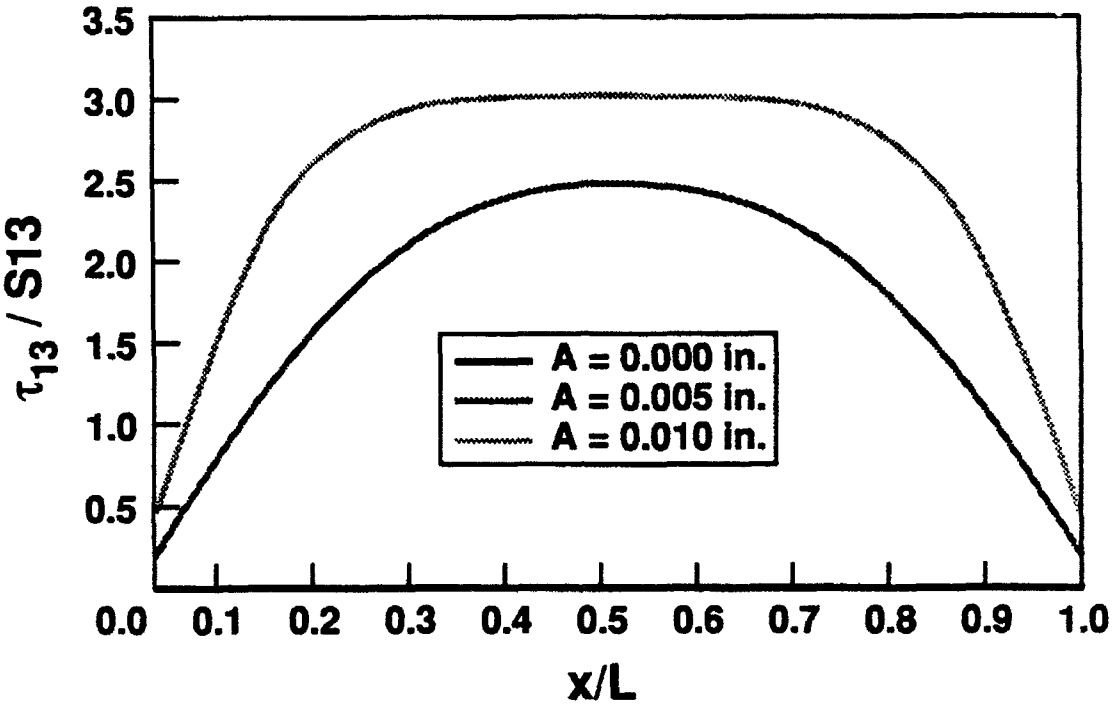

Figure 15. Interlaminar Shear Stress Within a Wavy [0] Ply in AS4 Graphite/PEK[illegible]: Uniaxial Loading (TR = 2, L/h = 5, N_x (A = 0) = –901 lb/in at Failure).

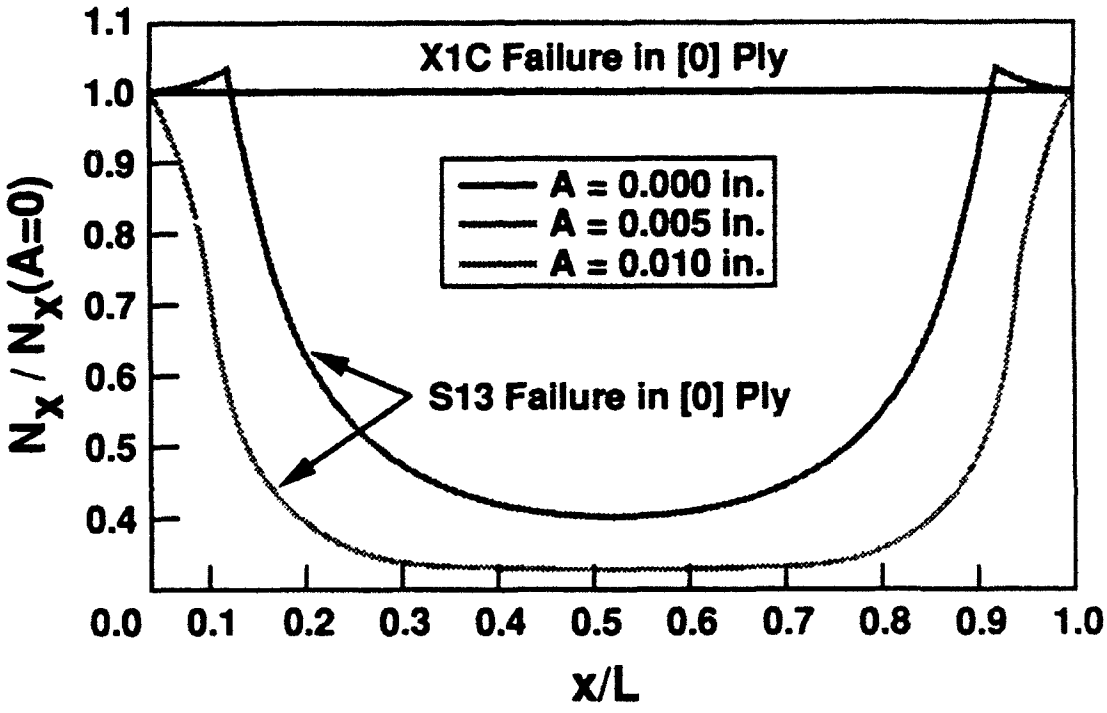

Figure 16. Strength Reduction in AS4 Graphite/PEKK: Uniaxial Loading (TR = 2, L/h_f = 5, N_x (A = 0) = –901 lb/in at Failure).

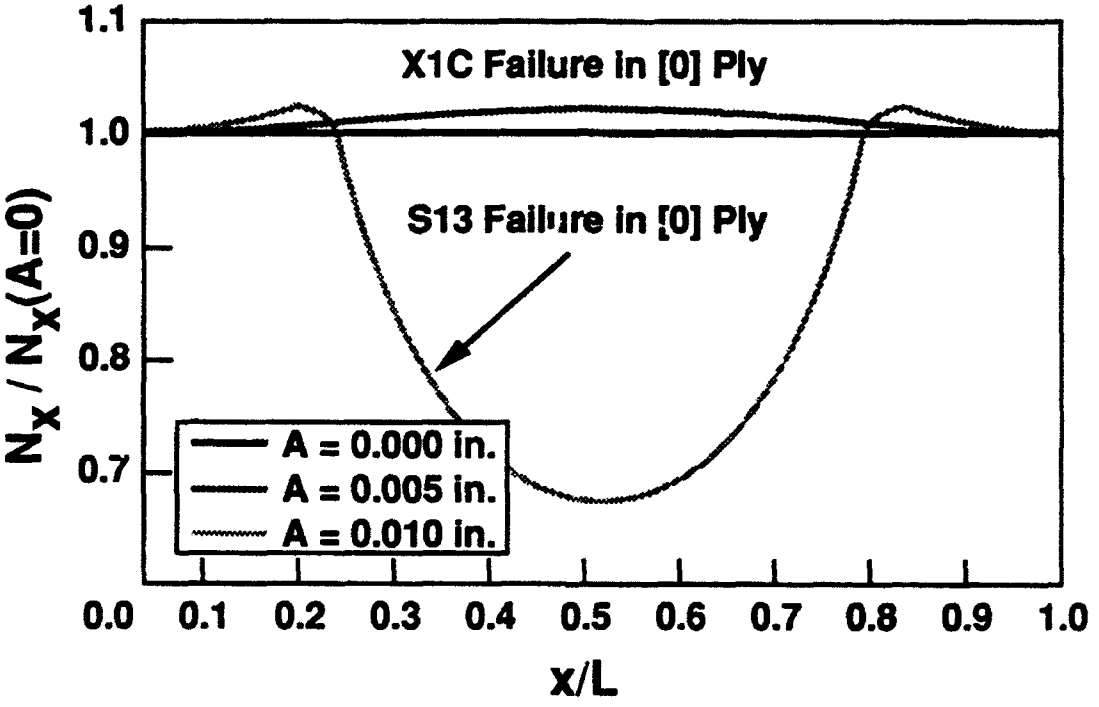

Figure 17. Strength Reduction in AS4 Graphite/PEKK: Uniaxial Loading ($TR = 2$, $L/h_f = 20$, N_x ($A = 0$) = –901 lb/in at Failure).

3.4.2 Biaxial Loading. Nondimensional failure envelopes for biaxial load conditions with and without thermal loading were generated to quantify the influence of ply waviness on strength reduction. The uniaxial stress resultants used to nondimensionalize the biaxial failure envelopes presented here are N_x ($A = 0$) = -901 lb/in at failure and N_y ($A = 0$) = -1,612 lb/in. The influence of ply undulation on strength reduction without thermal loading is illustrated in Figure 18. The plot indicates the y-direction strength is insensitive to ply waviness while x-direction strength can be substantially reduced (up to 35% for the particular ply configuration investigated). The same failure envelope, except with a thermal load of $\Delta T = -150°$ F, is presented in Figure 19. Since the thermal loading primarily influences the transverse stresses in the [90] plies, the addition of the thermal load has little affect on the ultimate strength of the applied loads.

The ultimate y-direction loading is defined almost exclusively by the longitudinal compressive strength allowable ($X1C$) of the [90] plies. In contrast, and consistent with the ply stress results presented earlier, the x-direction loading results in interlaminar shear failure ($S13$) in the [0] ply. This failure mechanism defines the right-hand side of the failure envelopes and is highly sensitive to the waviness of the [0] ply.

A major conclusion drawn from these results is that strength reduction in the direction of ply waviness is significant, highly sensitive to the degree of waviness, and is dominated by interlaminar shear failure in the wavy ply. Strength reduction in the non-wavy direction is relatively insignificant.

4. CONCLUSIONS

An analytical model was developed to quantify the influence of ply waviness on stiffness and strength reduction. The model provides an efficient design tool for accessing the synergistic effects of ply waviness on laminate stiffness and strength which can be directly related to structural performance. Parametric studies were conducted to identify the criticality of ply waviness on the stiffness and strength reduction of realistic composite structures.

Several significant findings were made. Stiffness reduction due to ply waviness is most significant in the direction of ply undulation. Other in-plane mechanical properties are relatively insensitive to ply waviness. The magnitude of stiffness reduction is extremely sensitive to the degree of ply waviness. Increasing undulation amplitude and decreasing unit cell length both increase observed stiffness reduction. Greater stiffness reduction can be expected in systems with higher material anisotropy (i.e., $E_2/E_1 << 1$).

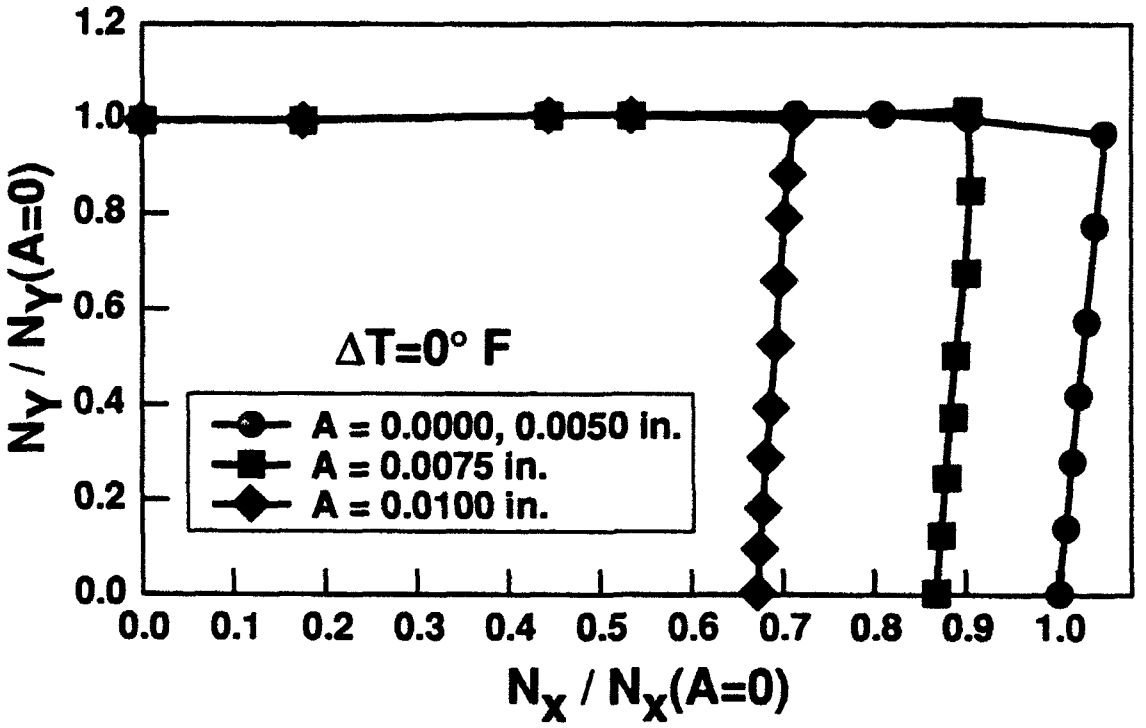

Figure 18. Nondimensional Biaxial Compression Failure Envelopes in AS4 Graphite/PEKK ($TR = 2$, $L/h_f = 20$, $\Delta T = 0°$ F, N_x ($A = 0$) = –901 lb/in, N_y ($A = 0$) = –1,612 lb/in).

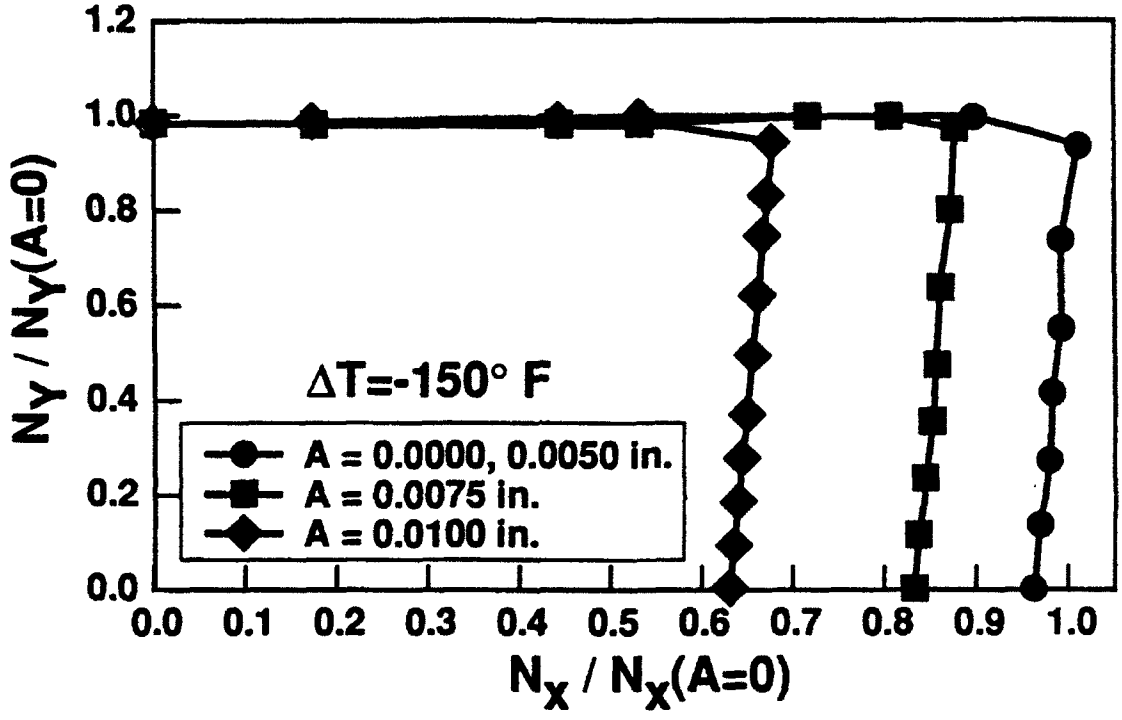

Figure 19. Nondimensional Biaxial Compression Failure Envelopes in AS4 Graphite/PEKK ($TR = 2$, $L/h_f = 20$, $\Delta T = -150°$ F, N_x ($A = 0$) = -901 lb/in, N_y ($A = 0$) = -1,612 lb/in).

Dominant failure mechanisms governing ultimate failure in wavy plies and the influence of ply waviness on strength reduction were also quantified. The most significant strength reduction results from interlaminar shear failure of the wavy ply when loaded in the direction of undulation. Strength reduction is extremely sensitive to the degree of ply waviness. Failures associated with loading transverse to the direction of undulation were unaffected by the degree of ply waviness. Failures associated with loading transverse to the direction of undulation were unaffected by the degree of ply waviness and were essentially the same as straight laminate failure loads.

The analysis developed in this work plays an important role in the design of composite structures where ply waviness cannot be ignored. The design procedure should employ the predicted reduced stiffness properties associated with the manufactured ply waviness into a suitable global stress analysis. The resulting global stress predictions should then be incorporated back into the failure analysis developed in this work to provide realistic estimates of the strength reduction to be expected. Predicted stiffness and strength reduction due to ply waviness represents one mechanism that may explain why design and failure analysis of thick-sectioned composite structures based on flat, autoclave-cured coupon property data do not correlate well with test results.

5. REFERENCES

Adams, D. O., and M. W. Hyer. "Effects of Layer Waviness on Compression-Loaded Thermoplastic Composite Laminates." Technical Report, CCMS-92-06/VPI-E-92-06, Center for Composite Materials and Structures, Virginia Polytechnic Institute and State University, Blacksburg, VA, 1992.

Argon, A. S. "Fracture of Composites." Treatise on Materials Science and Technology, vol.1, pp. 106-114, 1972.

Budiansky, B. "Micromechanics." Computers and Structures, vol. 16, no. 1–4, pp. 3–12, 1983.

Davis, J. G., Jr.. "Compressive Strength of Fiber-Reinforced Composite Materials." Composite Reliability, ASTM STP 580, American Society for Testing and Materials, Philadelphia, PA, pp. 364–377, 1975.

Garala, H. J. "Structural Evaluation of 8-Inch Diameter Graphite-Epoxy Composite Cylinders Subjected to External Hydrostatic Compressive Loading." Technical Report, DTRC-89/016, David Taylor Research Center, Bethesda, MD, 1989.

Hyer, M. W. "Micromechanics of Compression in Unidirectional Composites." Technical Report 86-9, Mechanical Engineering Department, University of Maryland, College Park, MD, August 1986.

Hyer, M. W., L. C. Maas, and H. P. Fuchs. "The Influence of Layer Waviness on the Stress State in Hydrostatically Loaded Cylinders." Journal of Reinforced Plastics and Composites, vol. 7, no. 11, pp. 601–613, 1988.

Ishikawa, T., and T. W. Chou. "Elastic Behavior of Woven Hybrid Composites." Journal of Composite Materials, vol. 16, pp. 2–19, 1982.

Ishikawa, T., and T. W. Chou. "In-Plane Thermal Expansion and Thermal Bending Coefficients of Fabric Composites." Journal of Composite Materials, vol. 17, pp. 92–104, 1983a.

Ishikawa, T., and T. W. Chou. "Nonlinear Behavior of Woven Fabric Composites." Journal of Composite Materials, vol. 17, pp. 399–413, 1983b.

Ishikawa, T., and T. W. Chou. "Thermoelastic Analysis of Hybrid Fabric Composites." Journal of Material Science, vol. 18, pp. 2260–2268, 1983c.

Jortner, J. "A Model for Predicting Thermal and Elastic Constants of Wrinkled Regions in Composite Materials." Effects of Defects in Composite Materials, ASTM STP 836, American Society for Testing and Materials, pp. 217–236, 1984.

Martinez, G. M., M. R. Piggott, D. M. R. Bainbridge, and B. Harris. "The Compression Strength of Composites With Kinked, Misaligned, and Poorly Adhering Fibers." Journal of Materials Science, vol. 16, pp. 2831–2836, 1981.

Peel, L. D. "Compression Failure of Angle-Ply Laminates." M.S. Thesis, Department of Engineering Science and Mechanics, Virginia Polytechnic Institute and State University, Blacksburg, VA, 1990.

Rosen, B. W. "Mechanics of Composite Strengthening." Fiber Composite Materials, American Society for Metals, Metals Park, OH, chap. 3, 1965.

Shuart, M. J. "Short-Wavelength Buckling and Shear Failures for Compression-Loaded Composite Laminates." Technical Report, NASA-TM-87640, National Aeronautics and Space Administration, Washington, D.C., 1985.

Shuart, M. J. "Failure of Compression-Loaded Multi-Directional Composite Laminates." AIAA Journal, vol. 27, no. 9, pp. 1274–1279, 1989.

Steif, P. S. "A Model for Kinking in Fiber Composites - I. Fiber Breakage via Micro-Buckling." International Journal of Solids and Structures, vol. 26, no. 5–6, pp. 549–561, 1990a.

Steif, P. S. "A Model for Kinking in Fiber Composites - II. Kink-Band Formation." International Journal of Solids and Structures, vol. 26, no. 5–6, pp. 563–569, 1990b.

Telegadas, H. K., and M. W. Hyer. "The Influence of Layer Waviness on the Stress State in Hydrostatically Loaded Cylinders: Further Results." Journal of Reinforced Plastics and Composites, vol. 9, no. 5, pp. 503–518, 1990.

Whitney, J. M. Structural Analysis of Laminated Anisotropic Plates, Technomic Publishing, 1987.

Whitney, J. M., I. M. Daniel, and R. B. Pipes. Experimental Mechanics of Fiber Reinforced Composite Materials, Prentice-Hall, 1982.

No. of Copies	Organization
2	Administrator Defense Technical Info Center ATTN: DTIC-DDA Cameron Station Alexandria, VA 22304-6145
1	Commander U.S. Army Materiel Command ATTN: AMCAM 5001 Eisenhower Ave. Alexandria, VA 22333-0001
1	Director U.S. Army Research Laboratory ATTN: AMSRL-OP-CI-AD, Tech Publishing 2800 Powder Mill Rd. Adelphi, MD 20783-1145
2	Commander U.S. Army Armament Research, Development, and Engineering Center ATTN: SMCAR-IMI-I Picatinny Arsenal, NJ 07806-5000
2	Commander U.S. Army Armament Research, Development, and Engineering Center ATTN: SMCAR-TDC Picatinny Arsenal, NJ 07806-5000
1	Director Benet Weapons Laboratory U.S. Army Armament Research, Development, and Engineering Center ATTN: SMCAR-CCB-TL Watervliet, NY 12189-4050
(Unclass. only) 1	Commander U.S. Army Rock Island Arsenal ATTN: SMCRI-IMC-RT/Technical Library Rock Island, IL 61299-5000
1	Director U.S. Army Aviation Research and Technology Activity ATTN: SAVRT-R (Library) M/S 219-3 Ames Research Center Moffett Field, CA 94035-1000

No. of Copies	Organization
1	Commander U.S. Army Missile Command ATTN: AMSMI-RD-CS-R (DOC) Redstone Arsenal, AL 35898-5010
1	Commander U.S. Army Tank-Automotive Command ATTN: ASQNC-TAC-DIT (Technical Information Center) Warren, MI 48397-5000
1	Director U.S. Army TRADOC Analysis Command ATTN: ATRC-WSR White Sands Missile Range, NM 88002-5502
1	Commandant U.S. Army Field Artillery School ATTN: ATSF-CSI Ft. Sill, OK 73503-5000
(Class. only) 1	Commandant U.S. Army Infantry School ATTN: ATSH-CD (Security Mgr.) Fort Benning, GA 31905-5660
(Unclass. only) 1	Commandant U.S. Army Infantry School ATTN: ATSH-CD-CSO-OR Fort Benning, GA 31905-5660
1	WL/MNOI Eglin AFB, FL 32542-5000
	Aberdeen Proving Ground
2	Dir, USAMSAA ATTN: AMXSY-D AMXSY-MP, H. Cohen
1	Cdr, USATECOM ATTN: AMSTE-TC
1	Dir, ERDEC ATTN: SCBRD-RT
1	Cdr, CBDA ATTN: AMSCB-CI
1	Dir, USARL ATTN: AMSRL-SL-I
10	Dir, USARL ATTN: AMSRL-OP-CI-B (Tech Lib)

No. of Copies	Organization
11	Director Benet Weapons Laboratory U.S. Army Armament Research, Development, and Engineering Center ATTN: SMCAR-CCB, J. Keane T. Allen J. Vasilakis G. Friar J. Zweig L. Johnson T. Simkins V. Montvori J. Wrzochalski G. D'Andrea R. Hasenbein Watervliet, NY 12189
7	Commander U.S. Army Armament Research, Development, and Engineering Center ATTN: SMCAR-CCH-T, S. Musalli P. Christian K. Fehsal SMCAR-CCH-V, E. Fennell SMCAR-CCH, J. DeLorenzo SMCAR-CC, R. Price J. Hedderich Picatinny Arsenal, NJ 07806-5000
2	Commander U.S. Army Armament Research, Development, and Engineering Center ATTN: SMCAR-TD, V. Linder T. Davidson Picatinny Arsenal, NJ 07806-5000
1	Commander Production Base Modernization Activity U.S. Army Armament Research, Development, and Engineering Center ATTN: AMSMC-PBM-K Picatinny Arsenal, NJ 07806-5000

No. of Copies	Organization
1	Commander U.S. Army Belvoir RD&E Center ATTN: STRBE-JBC, C. Kominos Fort Belvoir, VA 22060-5606
1	Commander U.S. Army Missile Command ATTN: AMSMI-RD, W. McCorkle Redstone Arsenal, AL 35898
3	Commander U.S. Army Armament Research, Development, and Engineering Center ATTN: SMCAR-FSA-M, R. Botticelli F. Diorio SMCAR-FSA, C. Spinelli Picatinny Arsenal, NJ 07806-5000
3	Project Manager Advanced Field Artillery System ATTN: COL Napoliello LTC A. Ellis G. DelCoco Picatinny Arsenal, NJ 07806-5000
1	Commander Watervliet Arsenal ATTN: SMCWV-QA-QS, K. Insco Watervliet, NY 12189-4050
2	Project Manager SADARM Picatinny Arsenal, NJ 07806-5000
2	PEO-Armaments ATTN: SFAE-AR-PM, D. Adams T. McWilliams Picatinny Arsenal, NJ 07806-5000
2	Commander Wright-Patterson Air Force Base ATTN: AFWAML, J. Whitney R. Kim Dayton, OH 45433

No. of Copies	Organization
8	Project Manager Tank Main Armament Systems ATTN: SFAE-AR-TMA, COL Hartline SFAE-AR-TMA-MD, C. Kimker H. Yuen R. Joinson J. McGreen SFAE-AR-TMA-ME, K. Russell D. Guzowitz SFAE-AR-TMA-MP, W. Lang Picatinny Arsenal, NJ 07806-5000
1	U.S. Army Research Office ATTN: A. Crowson P.O. Box 12211 Research Triangle Park, NC 27709-2211
1	Office of Naval Research Mechanical Division Code 1132-SM ATTN: Y. Rajapakse Arlington, VA 22217
1	Commander DARPA ATTN: J. Kelly 3701 North Fairfax Dr. Arlington, VA 22203-1714
2	Director U.S. Army Materials Technology Laboratory ATTN: SLCMT-MEC, B. Halpin T. Chou Watertown, MA 02172-0001
1	Naval Research Laboratory Code 6383 ATTN: Dr. I. Wolock Washington, DC 20375-5000
2	David Taylor Research Center ATTN: R. Rockwell W. Phyillaier Bethesda, MD 20054-5000
1	David Taylor Research Center Ship Structures and Protection Dept. ATTN: Dr. J. Corrado, Code 1702 Bethesda, MD 20084
4	Director Lawrence Livermore National Laboratory ATTN: R. Christensen S. deTeresa W. Feng F. Magness P.O. Box 808 Livermore, CA 94550
2	Pacific Northwest Laboratory A Div of Battelle Memorial Inst. Technical Information Section ATTN: M. Smith M. Garnich P.O. Box 999 Richland, WA 99352
6	Director Sandia National Laboratories Applied Mechanics Dept., Division-8241 ATTN: C. Robinson G. Benedetti W. Kawahara K. Ferano D. Dawson P. Nielan P.O. Box 969 Livermore, CA 94550-0096
1	Director Los Alamos National Laboratory ATTN: D. Rabern MEE-13, Mail Stop J-576 P.O. Box 1633 Los Alamos, NM 87545
3	University of Delaware Center for Composite Materials ATTN: J. Gillespe B. Pipes M. Santare 201 Spencer Laboratory Newark, DE 19716

No. of Copies	Organization
2	North Carolina State University Civil Engineering Dept. ATTN: W. Rasdorf L. Spainhour P.O. Box 7908 Raleigh, NC 27696-7908
1	University of Utah Department of Mechanical and Industrial Engineering ATTN: S. Swanson Salt Lake City, UT 84112
1	Stanford University Department of Aeronautics and Aeroballistics Durant Bldg. ATTN: S. Tsai Stanford, CA 94305
1	Pennsylvania State University Department of Engineering Science and Mechanics ATTN: Richard McNitt 227 Hammond Building University Park, PA 16802
1	Pennsylvania State University ATTN: Rena S. Engel 245 Hammond Building University Park, PA 16802
1	Pennsylvania State University ATTN: David W. Jensen 233-N Hammond University Park, PA 16802
3	Alliant Techsystems, Inc. ATTN: C. Candland J. Bode K. Ward 5640 Smetana Dr. Minnetonka, MN 55343
1	University of Illinois at Urbana-Champaign National Center for Composite Materials Research 216 Talbot Laboratory ATTN: J. Economy 104 South Wright Street Urbana, IL 61801
2	Olin Corporation Flinchbaugh Division ATTN: E. Steiner B. Stewart P.O. Box 127 Red Lion, PA 17356
1	Olin Corporation ATTN: L. Whitmore 10101 9th St., North St. Petersburg, FL 33702
1	Chamberlain Manufacturing Corporation Research and Development Division ATTN: T. Lynch 550 Esther Street P.O. Box 2335 Waterloo, IA 50704
1	Custom Analytical Engineering Systems, Inc. ATTN: A. Alexander Star Route, Box 4A Flintstone, MD 21530
2	Institute for Advanced Technology ATTN: T. Kiehne H. Fair 4030-2 W. Braker Lane Austin, TX 78759
1	UCLA MANE Department, Engineering IV ATTN: H. T. Hahn Los Angeles, CA 90024-1597
2	Virginia Polytechnical Institute and State University Dept. of ESM ATTN: M. W. Hyer K. L. Reifsnider Blacksburg, VA 24061-0219

No. of Copies	Organization
2	University of Dayton Research Institute ATTN: R. Y. Kim A. K. Roy 300 College Park Ave. Dayton, OH 45469-0168
1	University of Dayton ATTN: J. M. Whitney 300 College Park Ave. Dayton, OH 45469-0240
1	University of Kentucky ATTN: L. Penn 763 Anderson Hall Lexington, KY 40506-0046
1	Purdue University School of Aeronautics and Astronautics ATTN: C. T. Sun West Lafayette, IN 47907-1282
1	Drexell University ATTN: Albert S.D. Wang 32nd and Chestnut St. Philadelphia, PA 19104
2	Kaman Sciences Corporation ATTN: D. Elder J. Betz P.O. Box 7463 Colorado Springs, CO 80933

INTENTIONALLY LEFT BLANK.

USER EVALUATION SHEET/CHANGE OF ADDRESS

This Laboratory undertakes a continuing effort to improve the quality of the reports it publishes. Your comments/answers to the items/questions below will aid us in our efforts.

1. ARL Report Number ARL-TR-110 Date of Report April 1993

2. Date Report Received _____

3. Does this report satisfy a need? (Comment on purpose, related project, or other area of interest for which the report will be used.) _____

4. Specifically, how is the report being used? (Information source, design data, procedure, source of ideas, etc.) _____

5. Has the information in this report led to any quantitative savings as far as man-hours or dollars saved, operating costs avoided, or efficiencies achieved, etc? If so, please elaborate. _____

6. General Comments. What do you think should be changed to improve future reports? (Indicate changes to organization, technical content, format, etc.) _____

CURRENT ADDRESS

_____
Organization

_____
Name

_____
Street or P.O. Box No.

_____
City, State, Zip Code

7. If indicating a Change of Address or Address Correction, please provide the Current or Correct address above and the Old or Incorrect address below.

OLD ADDRESS

_____
Organization

_____
Name

_____
Street or P.O. Box No.

_____
City, State, Zip Code

(Remove this sheet, fold as indicated, tape closed, and mail.)
(DO NOT STAPLE)

DEPARTMENT OF THE ARMY

OFFICIAL BUSINESS

BUSINESS REPLY MAIL
FIRST CLASS PERMIT No 0001, APG, MD

Postage will be paid by addressee.

Director
U.S. Army Research Laboratory
ATTN: AMSRL-OP-CI-B (Tech Lib)
Aberdeen Proving Ground, MD 21005-5066

NO POSTAGE
NECESSARY
IF MAILED
IN THE
UNITED STATES